International Journal of Chronic Obstructive Pulmonary Disease

Dovepress
Taylor & Francis Group

Open Access Full Text Article

ORIGINAL RESEARCH

Identification of *CD14* as a Potential Biomarker Relating to PANoptosis in Chronic Obstructive Pulmonary Disease

Xue Fu[1], Jiawei Dong[2], Jian Yang[2], Xiaotian Zhang[2], Shangkun Cai[2], Yiwei Zhang[2], Shenglong Lv[2], Meng Zhang[2]

[1]Department of Emergency, Hebei Medical University Third Hospital, Shijiazhuang, 050051, People's Republic of China; [2]Department of Thoracic Surgery, Hebei Medical University Third Hospital, Shijiazhuang, 050051, People's Republic of China

Correspondence: Meng Zhang, Department of Thoracic Surgery, Hebei Medical University Third Hospital, No. 139 Ziqiang Road, Qiaoxi District, Shijiazhuang, 050051, People's Republic of China, Email 38000435@hebmu.edu.cn

Background: The processes of pyroptosis, apoptosis, and necroptosis (PANoptosis) play a crucial role in the development of chronic obstructive pulmonary disease (COPD). Our objective is to explore potential PANoptosis-related genes in COPD.

Methods: Human COPD-related transcriptomic datasets (GSE8545, GSE20257, GSE11784 and GSE1650) were retrieved from the Gene Expression Omnibus (GEO). First, based on GSE8545 dataset, candidate genes were identified using differentially expressed gene (DEG) analysis, Weighted Gene Co-expression Network Analysis (WGCNA), Least Absolute Shrinkage and Selection Operator (LASSO) regression, and Support Vector Machine-Recursive Feature Elimination (SVM-RFE). Subsequently, Gene Ontology (GO) and Kyoto Encyclopedia of Genes and Genomes (KEGG) pathway enrichment analyses were conducted for the relevant genes. *CD14* was identified as a diagnostic biomarker through validation across independent human cohorts (GSE20257 and GSE11784). CIBERSORT was employed to evaluate immune infiltration differences between *CD14* expression groups. Finally, potential therapeutic drugs for *CD14* were predicted using the Drug-Gene Interaction Database (DGIdb).

Results: Three PANoptosis-related hub genes (*CD14, IRF2*, and *BOK*) were defined in this study. KEGG enrichment analysis revealed that these genes were significantly enriched in the "Apoptosis - multiple species" signaling pathway. Validation across multiple independent human datasets identified *CD14* as the key gene. *CD14* exhibited significantly elevated expression in the lung tissues of COPD patients ($P < 0.001$). Immune infiltration analysis indicated that *CD14* expression levels were significantly negatively correlated with resting mast cells and positively correlated with monocytes. Receiver Operating Characteristic curve analysis confirmed the robust diagnostic performance and stability of *CD14*, with Area Under the Curve values of 0.756, 0.702, 0.703, and 0.732 in the GSE8545, GSE20257, GSE11784, and GSE1650 datasets, respectively. Furthermore, three potential therapeutic agents targeting *CD14*—VB-201, LOVASTATIN, and IC143—were predicted.

Conclusion: We identified *CD14* as a marker gene associating with PANoptosis in COPD, providing new ideas for clinical diagnosis and drug design of COPD.

Keywords: COPD, PANoptosis, immune infiltration, target drugs, *CD14*

Introduction

Chronic obstructive pulmonary disease (COPD) is a chronic inflammatory condition characterized by persistent airway inflammation. It typically progresses over several years, leading to substantial morbidity and mortality.[1–3] Worldwide, the prevalence of COPD among individuals aged 30–79 years ranges from 7.6% to 10.6%.[4] COPD patients face a heightened risk of developing lung cancer and other comorbidities compared to healthy individuals.[5] Given this context, early diagnosis and effective intervention are of paramount clinical importance for improving the overall survival rate of COPD patients. Consequently, there has been significant interest in identifying biomarkers for COPD over the past few decades. For example, through single-cell RNA sequencing (scRNA-seq), *IGFBP5* serves as a signature gene for ciliated

https://doi.org/10.2147/COPD.S577042
Received: 27 October 2025
Accepted: 14 April 2026
Published: 1 May 2026

epithelial cells in COPD, playing a pivotal causal role in driving cellular senescence, inflammatory responses, and airway remodeling.[6] Using mass spectrometry analysis of metabolomics, Richard et al searched for new predictive biomarkers associated with COPD.[7] Recently, Zhong et al provided a theoretical basis for linking aging effectors to COPD progression.[8] Therefore, identifying biomarkers associated with the pathogenesis of COPD has emerged as a major research focus in recent years.

Apoptosis, pyroptosis, and necroptosis are recognized as the core pathophysiological mechanisms underlying the onset and progression of COPD.[9–11] As a fundamental process for maintaining tissue homeostasis, apoptosis is triggered by persistent oxidative stress and inflammatory mediators; however, excessive apoptosis leads to the loss of epithelial and endothelial cells, thereby compromising the integrity and function of lung tissue.[12] Pyroptosis is a highly pro-inflammatory form of programmed cell death, typically activated by inflammasomes. It is characterized by persistent cell swelling that leads to plasma membrane rupture and the release of a large amount of inflammatory cytokines, which subsequently exacerbates pathological damage in COPD.[13,14] Necroptosis is a molecularly regulated form of "controlled necrosis", usually triggered by the RIPK1/RIPK3/MLKL protein complex when apoptosis is inhibited.[15] This leads to cell membrane perforation and the leakage of cellular contents, which likewise induces a strong inflammatory response.[15] Previous studies have demonstrated that within the pathological context of COPD, necroptosis mediates cigarette smoke-induced pulmonary epithelial inflammation by promoting the extracellular release of damaged mitochondrial DNA, serving as a key mechanism driving the progression of COPD.[16] However, apoptosis, pyroptosis and necroptosis do not function as isolated processes.[17] Recent studies have demonstrated intimate signaling crosstalk and synergy among these three pathways. This integrated network, composed of multiple cell death pathways, is defined as PANoptosis, representing a more advanced form of regulated cell death in response to complex environmental stress.[18]

PANoptosis is a newly defined and highly integrated programmed cell death mode. It is not merely a simple juxtaposition of apoptosis, pyroptosis, and necroptosis. Instead, it organically integrates key molecules from these three signaling pathways, such as RIPK1 and Caspase-8, through the formation of a large multi-protein complex called the PANoptosome.[19,20] This mechanism allows cells to synergistically trigger multiple death pathways upon exposure to pathogens or inflammatory stimuli, thereby generating a more robust inflammatory response.[21] PANoptosis has been linked to various inflammatory diseases.[22–24] It has been reported that RIPK1 kinase activity drives activation of the NLRP3 inflammasome and PANoptosis, which could be targeted for the treatment of TAK1-associated myeloid proliferation and septicemia.[24] In rats with sepsis-related encephalopathy, inhibiting TLR9 has been indicated to lead to the suppression of the MAPK pathway, thereby suppressing PANoptosis and improving the survival rate of the affected animals.[25] In addition, there is growing evidence that PANoptosis is involved in the pathogenesis of pulmonary disease.[26,27] The inhibition of PANoptosis provided protection for mice from COVID-19-induced acute lung damage.[28] Yasmine et al demonstrated that stimulators of interferon genes agonists induced acute respiratory distress syndrome by PANoptosis.[29] Nisa et al have summarized different patterns of host cell death mediated by Mycobacterium tuberculosis, including PANoptosis.[30] Therefore, understanding the mechanisms of PANoptosis is crucial for developing effective therapeutic strategies for various human diseases. However, to the best of our knowledge, reports on COPD-specific PANoptosis are limited. While PANoptosis has been implicated in the pathogenesis of various inflammatory disorders, its clinical significance in COPD remains largely unexplored. The ability of PANoptosis to integrate multiple programmed cell death pathways and drive robust inflammatory responses aligns closely with the persistent chronic inflammation characteristic of COPD. Therefore, this study aims to investigate the connection between these two conditions and identify core PANoptosis-related genes (PANRGs) that may serve as novel diagnostic biomarkers for COPD.

In this study, our primary objective is to identify robust PANoptosis-related hub genes in COPD using integrated bioinformatic approaches, aiming to establish highly reliable diagnostic biomarkers. Subsequently, we explore the correlation between these core genes and the infiltration of the lung immune microenvironment, alongside predicting potential targeted therapeutic agents, to provide a scientific reference for the precision medicine of COPD. The overall analytic workflow is illustrated in Figure 1.

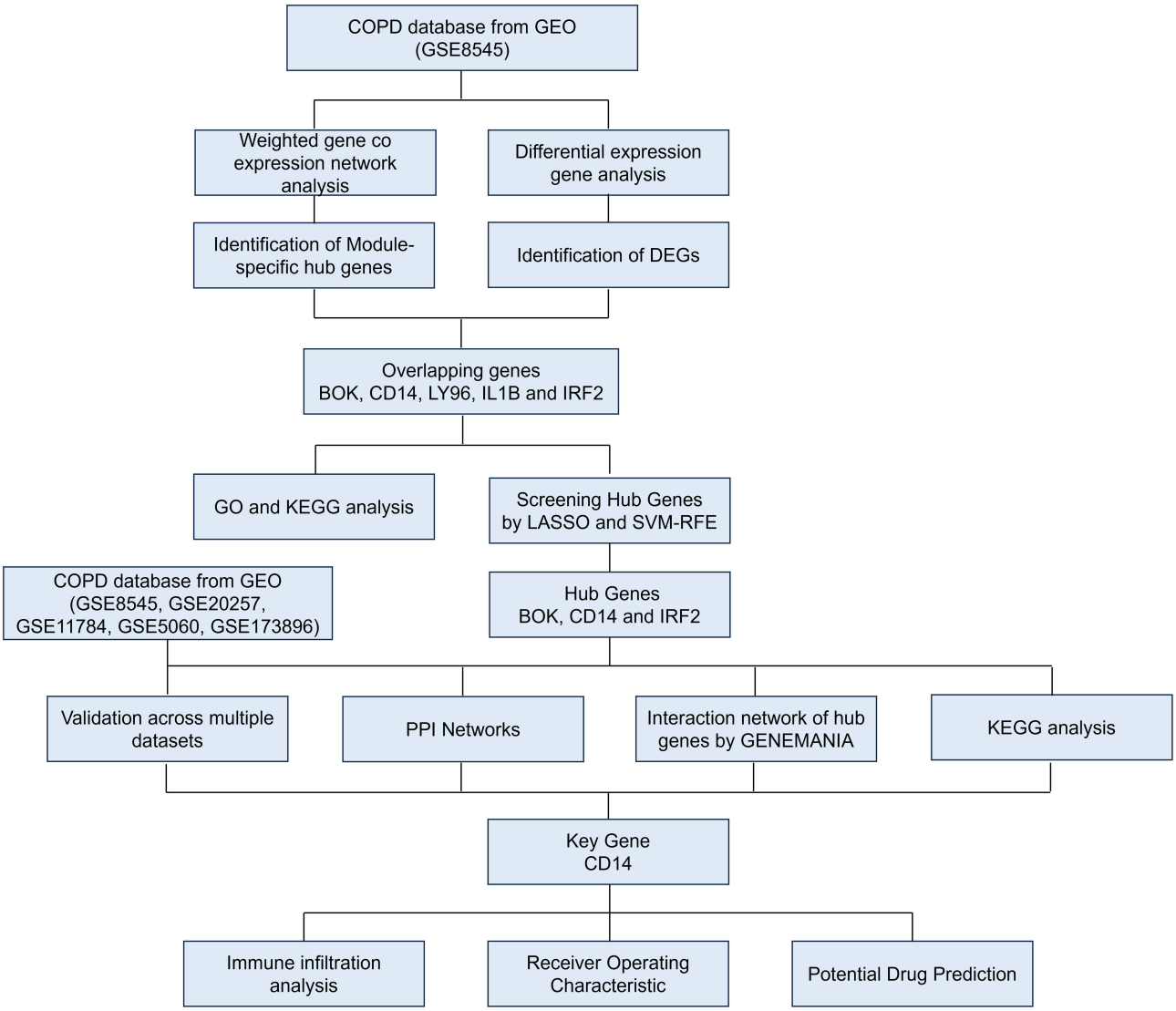

Figure 1 Flowchart for research.

Materials and Methods

Subjects

The human mRNA expression profile datasets GSE8545 (18 COPD samples and 18 control samples), GSE20257 (23 COPD samples and 59 control samples), GSE11784 (22 COPD samples and 72 control samples), and GSE1650 (18 COPD samples and 12 control samples) were downloaded from the Gene Expression Omnibus (GEO) database (https://www.ncbi.nlm.nih.gov/geo/). The COPD cohorts specifically included samples from current smokers diagnosed according to the Global Initiative for Chronic Obstructive Lung Disease (GOLD) I or II criteria.[31–33] In this study, the control group consists of non-COPD smokers obtained from the public datasets. GEO is a robust, public functional genomics data repository maintained by the National Center for Biotechnology Information, which supports the archiving and distribution of high-throughput gene expression datasets generated by gene chips, next-generation sequencing, and other functional genomic techniques. The datasets GSE8545, GSE20257, and GSE11784 were obtained using the Affymetrix Human Genome U133 Plus 2.0 Array platform. Following data download, probe information was converted into Gene Symbols based on the platform's annotation files to facilitate subsequent analysis. Besides, a scRNA-seq data set GSE173896 was also downloaded from the GEO database, 5 COPD samples and 2 control samples were selected from GSE173896.

Weighted Gene Co-Expression Network Analysis (WGCNA)

WGCNA was performed based on the expression values of the top 25% genes—screened by median absolute difference—using the "WGCNA" function package (version1.72–1)[34] of R software. WGCNA can characterize patterns of genetic association between different samples for the identification of highly cooperative gene modules. Candidate markers can be identified based on the relationship between gene modules and phenotypes. Finally, we assessed the correlation between each module and the pathogenesis of COPD, and selected the significantly associated modules as the central gene modules derived from WGCNA. $p<0.05$ was considered with significant correlation.

Differential Gene Expression Analysis (DEGs)

DEGs were screened using "limma" package (version 3.52.4)[35] of R software with a threshold of $|\log_2 FC|> 0.5$ and p.adjust <0.05.

Functional Enrichment Analysis

The enrichment analysis of gene ontology (GO, including biological process (BP), molecular function (MF) and cellular component (CC)) and Kyoto Encyclopedia of Genes and Genomes (KEGG) pathway were performed using the "clusterProfiler" R package (version 4.7.1.2).[36] The significantly enriched GO term and KEGG pathway were screened using p.adjust <0.05 as a criterion.

Screening of the PANoptosis-Related Hub Genes

The hub genes related to PANoptosis in COPD were further screened using the intersection of support vector machine recursive feature elimination (SVM-RFE) and least absolute shrinkage and selection operator (LASSO). The SVM-RFE algorithm, implemented using the "e1071" R package (https://CRAN.R-project.org/package=e1071), was utilized to identify genes with high discriminatory power. Moreover, the LASSO analysis was performed using the "glmnet" package (version 4.1–8) of the R software,[37] which represented a regression analysis algorithm applying regularization for variable selection.

Protein–Protein Interaction (PPI) Analysis

The STRING database (version 11.0; https://string-db.org/), a comprehensive resource, was employed to explore PPI and their functional associations.[38] STRING is a comprehensive online resource designed to integrate both known and predicted physical interactions and functional associations between proteins, deriving information from experimental evidence, computational prediction methods, and public text mining. We utilized Cytoscape (version 3.7.2; https://cytoscape.org/) to visualize the PPI networks.[39]

To gain insights into the intricate interactions between proteins and assess potential biological pathways, we employed the online database GeneMANIA (http://www.genemania.org) to look for genes sharing functions.

scRNA-Seq Data Analysis

The processing of scRNA-seq data was carried out using the "Seurath" package (version 5.0.1) in R software.[40] Initially, the raw scRNA-seq data were filtered to eliminate low-quality single cells. This was followed by normalization of the remaining data using the "NormalizedData" function. Using "RunPCA" function, the principal component analysis (PCA) was conducted on the normalized data. Next, the "FindClusters" function in the "Seurat" package was utilized for unsupervised clustering of the major cell subtypes. The clusters were visualized using "umap" for manual annotation based on cell markers.

Analysis of the Immune Cell Infiltration

To calculate the relative abundances of the 22 immune cell types in every sample, we employed the CIBERSORT software.[41] This software employed a deconvolution algorithm and utilized a predefined set of 547 barcode genes to

assess the composition of infiltrating immune cells based on the gene expression matrix. Notably, the sum of all estimated immune cell type proportions in each sample was normalized to 1.

Targeted Drug Prediction for COPD

The Comparative Toxicogenomics Database (CTD, http://ctdbase.org/) offered comprehensive information on the intricate interactions between various chemical exposures (both environment and drugs), genes, proteins, phenotypes and diseases. This database was used to analyze the relationship between the key gene and COPD. Additionally, the Drug-Gene Interaction Database (DGIdb) (version 4.2.0-sha1 afd9f30b) (https://dgidb.genome.wust-l.edu) was employed for predicting drugs that targeted the gene.

Statistical Analysis

The differences in gene expression levels and immune cell infiltration among various groups were determined using the Mann–Whitney *U*-test. The Pearson correlation analysis was conducted using the "cor" function in the R software. To establish the diagnostic value of the marker gene, receiver operating characteristic (ROC) curves were constructed using the "pROC" R package (version 1.18.4).[42] Statistical significance was set at $p < 0.05$. All statistical analyses were performed using R software (version 4.3.1).

Results

Identification of DEGs in COPD

To identify potential biomarkers of COPD, differential expression analysis was performed between COPD and control samples using the GSE8545 dataset. After applying stringent criteria of an adjusted p value <0.05 and a $|\log_2 FC| > 0.5$, we identified a total of 11,648 DEGs in the COPD group compared to the control group, including 11,510 up-regulated genes and 138 down-regulated genes (Figure 2A and B).

We conducted GO and KEGG pathway enrichment analyses to gain insights into the potential function of these DEGs. The results revealed that 140 KEGG pathways, including Salmonella infection, Human T−cell leukemia virus 1 infection, Autophagy, and Apoptosis, were significantly enriched (Figure 2C), along with 2,154 GO terms. In the BP assessment, DEGs were mostly engaged in ribonucleoprotein complex binding and other functions. DEGs have been localized to the mitochondrial matrix, focal adhesion and other structures in CC. DEGs associated with MF include regulation of cadherin binding, GTPase binging and other functions. The top 10 most significantly enriched GO terms were shown in Figure 2D. Further details of the enrichment results are provided in Table S1.

Construction of WGCNA and Identification of COPD-Related Modules

DEG analysis was conducive to mine potential biomarkers of COPD from the perspective of differences, and the co-expression patterns of genes were also important. To identify the potential gene modules associated with COPD, WGCNA was conducted using the GSE8545 dataset. The soft threshold in this study was 5 (Figure 3A), and a sum of 9 distinct gene modules were revealed (Figure 3B and C). The trait data for WGCNA included sample type (COPD and control), age, and gender. The correlation between each gene module and traits was calculated (Figure 3D). Notably, totally four gene modules were significantly correlated with COPD (p-value <0.05), including pink (Figure 3E), brown (Figure 3F), turquoise (Figure 3G), and green (Figure 3H) modules, which contained a total of 3,583 genes.

Screening Candidate PANoptosis-Related Hub Genes in COPD

To more accurately identify candidate PANRGs in COPD, we retrieved 66 PANRGs including 26 pyroptosis-related genes, 32 apoptosis-related genes, and 8 necroptosis-related genes from a published study[43] (Figure 4A). Next, five overlapping genes including *BOK, CD14, LY96, IL1B, and IRF2* were generated by taking the intersection of the 11,648 DEGs, 3,583 WGCNA module-related genes, and 66 PANRGs (Figure 4B). KEGG pathway enrichment was performed to further explore the function of these five overlapping genes in COPD and the results showed that the overlapping

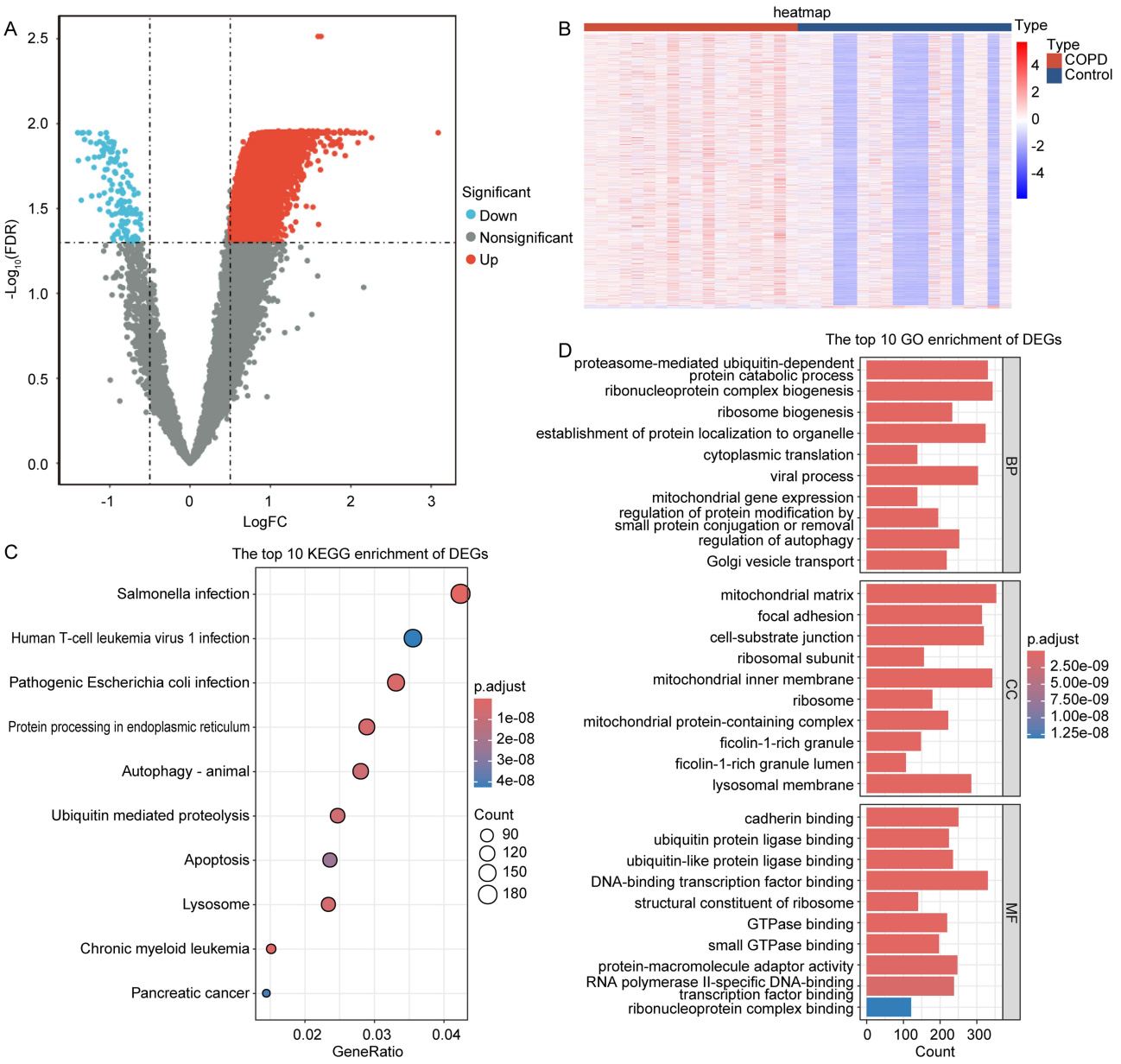

Figure 2 DEG analysis between the COPD and control samples and functional enrichment analysis in the GSE8545 cohort. (**A**) Volcano plot of DEGs. Red dots indicate up-regulated genes, blue dots indicate down-regulated genes, and gray dots represent genes with no significant difference. (**B**) Heatmap of the DEGs. (**C**) The top 10 KEGG pathways enrichment of DEGs. (**D**) The top 10 GO enrichment analysis of DEGs.

genes were significantly enriched in 12 KEGG pathways (Table 1), including Pertussis, NF-kappa B signaling pathway, Tuberculosis and other functions.

To further narrow down the pool of candidate PANRGs, LASSO regression and SVM-RFE algorithm were conducted. The LASSO regression algorithm successfully identified three genes (Figure 4C), while the SVM-RFE revealed five genes (Figure 4D). Finally, three genes including *BOK, CD14*, and *IRF2* were generated by intersecting the genes identified through both algorithms (Figure 4E).

A PPI network was constructed for these three hub genes using the STRING database to examine inter-gene relationships. Interaction pairs were filtered based on a minimum required interaction score > 0.15. Subsequently, the PPI network was visualized using Cytoscape software (Figure 4F). Additionally, the interplay networks for the hub genes were constructed using GENEMANIA (Figure 4G and Table S2). A total of 367 interaction pairs were identified,

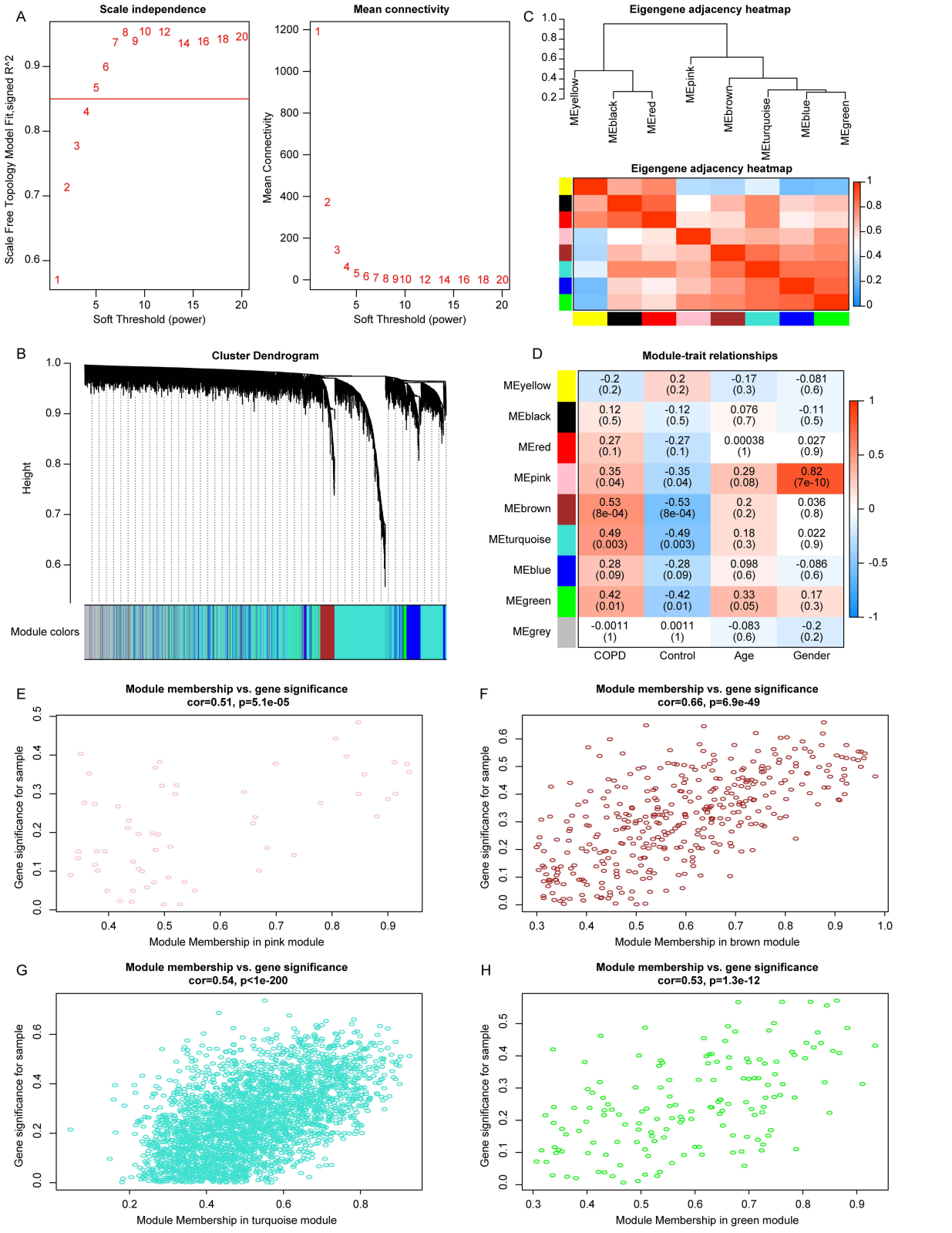

Figure 3 Identification of COPD-associated gene modules in the GSE8545 cohort using WGCNA. (**A**) Determination of the soft-threshold power. (**B**) Dendrogram of all genes in the GSE8545 dataset based on a topological overlap matrix. The upper half presents the hierarchical clustering dendrogram of genes, while the lower half visualizes the gene modules. Each color represents a distinct module, and the gray module signifies genes that cannot be aggregated to any other modules. (**C**) Eigengene adjacency heatmap. The gray module was excluded. (**D**) Heatmap of the correlation between modules and traits. The numbers in each cell indicate the correlation and *p* value. (**E**–**H**) Scatter plots of the correlation of genes with the pink, brown, turquoise, and green modules.

https://doi.org/10.2147/COPD.S577042

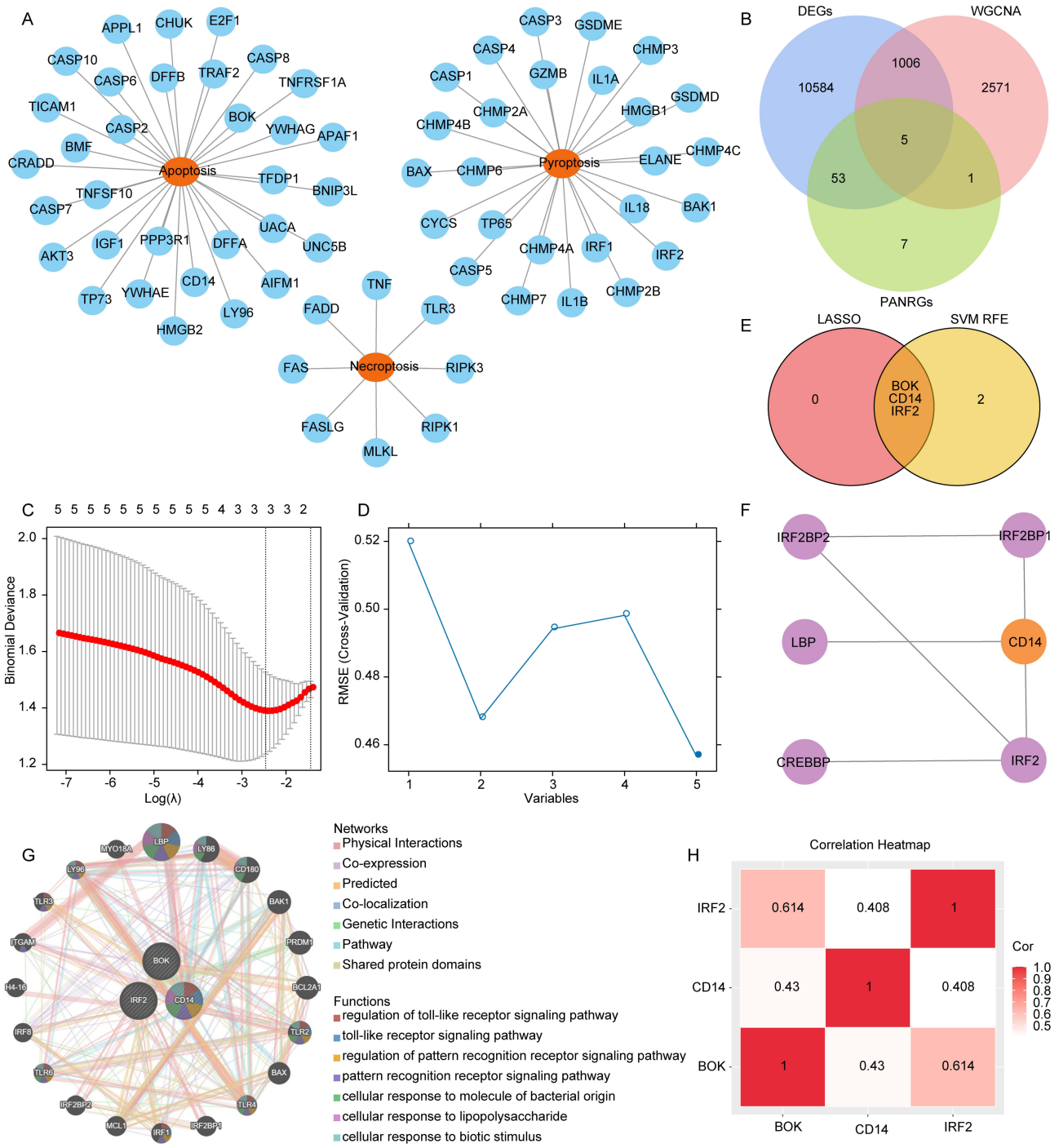

Figure 4 Screening candidate PANoptosis-related hub genes. (**A**) The network of downloaded 66 PANRGs from a published study. (**B**) Venn diagram of the WGCNA modules, DEGs, and PANRGs. (**C**) The cross-validation curve for the LASSO regression analysis. (**D**) The results of the screening of diagnostic markers by the SVM-RFE algorithm. (**E**) Venn diagram of LASSO and SVM-RFE algorithms. (**F**) PPI network interaction map of three hub genes including *BOK*, *CD14*, and *IRF2*, where a node represents a gene, and the edges represent their interrelationships. (**G**) Network interaction map of three hub genes based on GENEMANIA. (**H**) Correlation heatmap among the identified candidate hub genes.

including 80 co-expression, 12 co-localization, 20 genetic interactions, 138 physical interactions, 46 shared protein domains, 37 pathways, and 34 predicted, implying the complex crosstalk among the hub genes in COPD.

Correlation analysis revealed significant positive correlations among all three hub genes (Figure 4H). Additionally, KEGG pathway enrichment analysis was conducted on the three hub genes, revealing that they were enriched in 8 KEGG

Table 1 12 Pathway of KEGG Enrichment Analysis of Five PANoptosis-Related Genes

ID	Description	Bg Ratio	P value	P.adjust	Q value	Gene ID	Count
hsa05133	Pertussis	76/8659	2.58E-06	0.000119694	4.99E-05	929/23,643/3553	3
hsa04064	NF-kappa B signaling pathway	104/8659	6.68E-06	0.000119694	4.99E-05	929/23,643/3553	3
hsa04620	Toll-like receptor signaling pathway	108/8659	7.48E-06	0.000119694	4.99E-05	929/23,643/3553	3
hsa04936	Alcoholic liver disease	142/8659	1.71E-05	0.000204815	8.53E-05	929/23,643/3553	3
hsa05417	Lipid and atherosclerosis	215/8659	5.93E-05	0.000569192	0.000237163	929/23,643/3553	3
hsa05132	Salmonella infection	249/8659	9.20E-05	0.000736018	0.000306674	929/23,643/3553	3
hsa05134	Legionellosis	56/8659	0.000244454	0.001676259	0.000698441	929/3553	2
hsa04640	Hematopoietic cell lineage	99/8659	0.000764922	0.004329865	0.001804111	929/3553	2
hsa05146	Amoebiasis	102/8659	0.00081185	0.004329865	0.001804111	929/3553	2
hsa05152	Tuberculosis	180/8659	0.002508493	0.012040764	0.005016985	929/3553	2
hsa05131	Shigellosis	247/8659	0.00468137	0.020427795	0.008511581	929/3553	2
hsa04010	MAPK signaling pathway	301/8659	0.006898414	0.027593656	0.011497357	929/3553	2

Table 2 8 Pathway of KEGG Enrichment Analysis of Three Hub Genes

ID	Description	Bg Ratio	P value	P.adjust	Q value	Gene ID	Count
hsa04215	Apoptosis - multiple species	32/8659	0.007377922	0.049582003	0.009785922	666	1
hsa05134	Legionellosis	56/8659	0.012893436	0.049582003	0.009785922	929	1
hsa05221	Acute myeloid leukemia	67/8659	0.015416244	0.049582003	0.009785922	929	1
hsa05133	Pertussis	76/8659	0.017477959	0.049582003	0.009785922	929	1
hsa04640	Hematopoietic cell lineage	99/8659	0.022736969	0.049582003	0.009785922	929	1
hsa05146	Amoebiasis	102/8659	0.023421887	0.049582003	0.009785922	929	1
hsa04064	NF-kappa B signaling pathway	104/8659	0.023878365	0.049582003	0.009785922	929	1
hsa04620	Toll-like receptor signaling pathway	108/8659	0.024791001	0.049582003	0.009785922	929	1

pathways (Table 2), including Apoptosis-multiple species, Pertussis, and NF-kappa B signaling pathway. These results suggested that *BOK, CD14*, and *IRF2*, as candidate PANoptosis-related hub genes, may play a key role in the occurrence and progression of COPD.

Identification of CD14 as a PANoptosis-Related Key Gene in COPD

To ensure the reliability of the hub genes identified above, we validated their expression in various datasets. Initially, we analyzed the expression of the three hub genes using bulk datasets GSE8545, GSE20257, and GSE11784. We found that all three candidate genes were significantly up-regulated in COPD samples compared to control samples in the GSE8545 cohort (Figure 5A). Validation in the GSE20257 and GSE11784 datasets confirmed that *CD14* was significantly up-regulated in COPD samples; however, *BOK* and *IRF2* showed no significant differential expression (Figure 5B and C).

Additionally, to partly evaluate the contribution of hub genes to COPD progression, we compared the expression of the three hub genes in late-stage and early-stage COPD samples using the GSE5060 dataset. The results revealed that *BOK* expression was significantly higher in late-stage COPD samples compared to early-stage COPD samples. Meanwhile, *CD14* and *IRF2* both tended to exhibit higher expression in late-stage COPD samples, although the differences did not reach statistical significance (Figure 5D). We analyzed the correlation among these three genes in COPD patients at different stages. The results showed that the correlation was more pronounced in late-stage patients (Figure S1), while it was not significant in the early stage. This suggests that the potential interplay among these genes may be associated with disease progression.

Subsequently, the expression of genes *BOK, CD14*, and *IRF2* was also verified from the single cell resolution using the GSE173896 scRNA-seq dataset. We performed PCA using 5000 variable genes to reduce the dimensionality (Figure S2A). A total of 21 cell clusters were identified (Figure 5E), and 11 types of cells were annotated (Figure 5F), and the proportion of 11 cells in COPD and control samples were shown in Figure S2B. The results showed that the expressions

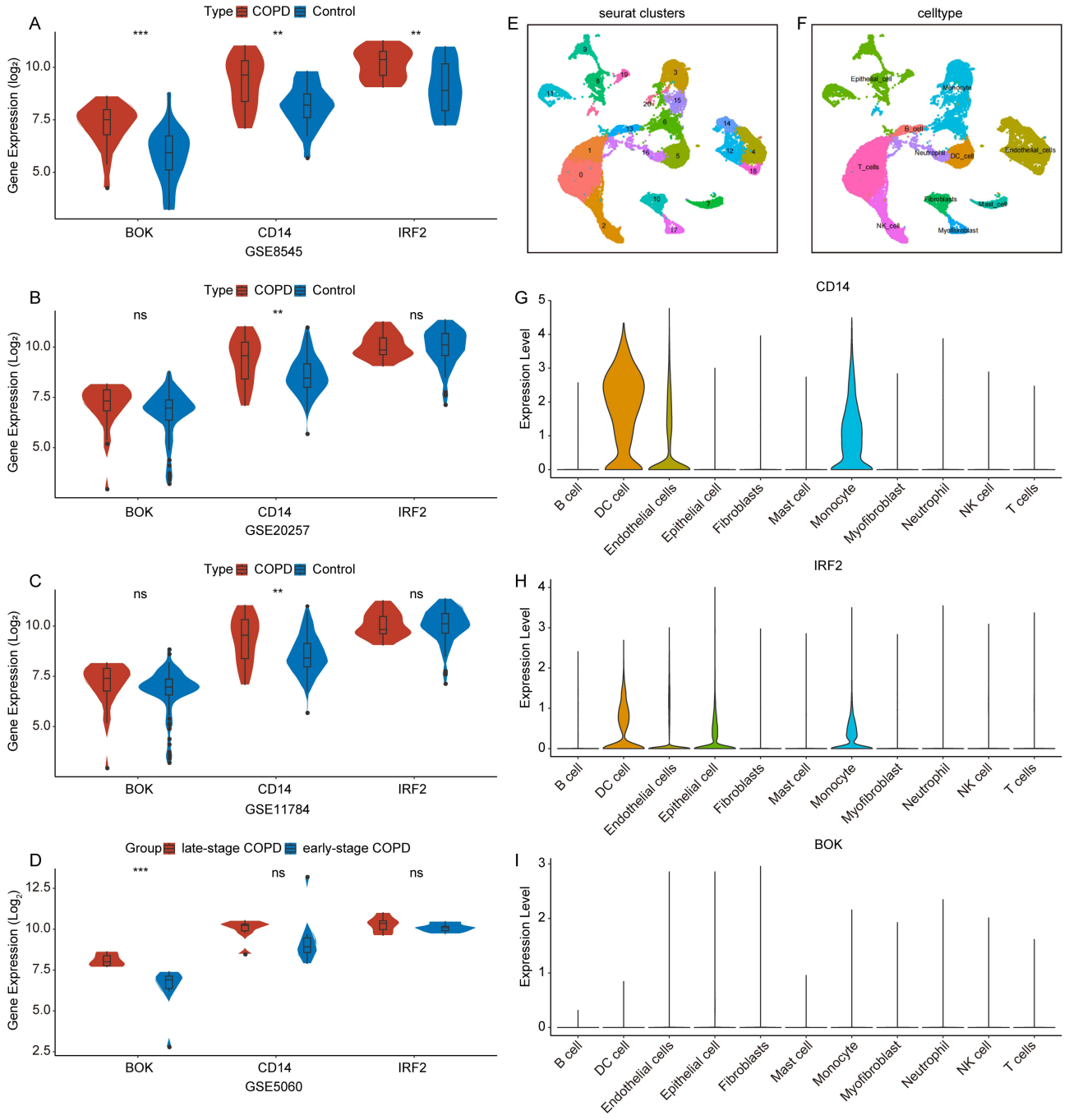

Figure 5 Identification of *CD14* as a PANoptosis-related key gene in COPD. (**A-C**) Violin plots of hub genes' expression in COPD and control samples from GSE8545 (A), GSE20257 (B), and GSE11784 cohorts (**C**). (**D**) Violin plots of candidate hub genes' expression in late-stage COPD and early-stage COPD samples in GSE5060 cohort. (**E**) 21 cell clusters were identified based on scRNA-seq data of 5 COPD and 2 control samples from GSE173896 dataset. (**F**) Classification results of cell clusters based on the umap algorithm and 11 immunological cell types were classified. (**G–I**) The expression of *CD14, IRF2*, and *BOK* in 11 immunological cell types. Statistical significance: **P < 0.01, ***P < 0.001; ns, not significant.

of *BOK, CD14*, and *IRF2* were relatively low in both COPD and control samples (Figure S2C) in the GSE173896 dataset. Thus, we analyzed the hub genes expressions in various cells. Among the immune cells, we noticed that *CD14* and *IRF2* exhibited distinct expression patterns across different immune cell types (Figure 5G and H), while *BOK* expression did not vary significantly (Figure 5I). Collectively, considering the consistent up-regulation across different levels, *CD14* was chosen as the key target in our subsequent studies.

Distinct Immune Cell Infiltration Between High and Low CD14 Expression COPD Patients

Since the differential expression of *CD14* in different immune cells was observed in the single-cell validation, we further refined the patient immune landscape to analyze the relationship between *CD14* and immune cells in COPD patients. We used the CIBERSORT algorithm to calculate the proportion of 22 immune cells in the GSE8545 cohort (Figure 6A). Based on the median expression value of *CD14*, the COPD samples in the cohort were divided into high *CD14* expression group and low *CD14* expression group. The differences in immune cell infiltration between these two groups were then analyzed. The results revealed that the proportions of plasma cells, T cells CD4 memory resting, and mast cells resting were significantly increased in the low *CD14* expression group in contrast to the high *CD14* expression group. On the contrary, the high *CD14* expression group showed a higher infiltration proportion of monocytes (Figure 6B).

To further investigate the relationship between *CD14* and these significantly different infiltrating immune cells, the Pearson correlation analysis was performed. The results showed a significant negative correlation between *CD14* and mast cells resting, T cells CD4 memory resting, plasma cells, and a significant positive correlation with monocytes (Figure 6C).

Going a step further, we calculated the proportion of immune cell infiltration between late-stage and early-stage COPD samples and observed that the proportion of T cells CD4 memory resting in late-stage COPD samples was significantly lower than in early-stage COPD samples (Figure 6D). These results suggested that the role of *CD14* in COPD inflammation may be mediated through the regulation of immune cells.

Mining of the Clinical Value of CD14 in COPD

To assess the diagnostic value of *CD14* in COPD, the ROC curves were plotted using the GSE8545, GSE20257, GSE11784 and GSE1650 datasets. The results demonstrated Area Under the Curve (AUC) values of 0.756, 0.702, 0.703 and 0.732 respectively across these four cohorts (Figure 7A–D). Furthermore, the ROC curves for early-stage and late-stage COPD samples were constructed utilizing the GSE5060 dataset, resulting in an AUC value of 0.759 (Figure 7E). These findings indicate that *CD14* exhibits favorable diagnostic performance as a biomarker for COPD.

In order to further validate the association between *CD14* and COPD, gene-inferred scores from the CTD database were analyzed which confirmed their correlation (Figure 7F). Moreover, potential drugs targeting *CD14* were predicted using the DGIdb database leading to the identification of three candidate drugs including VB-201, LOVASTATIN, and IC143 (Figure 7G).

Discussion

In this study, we compared COPD and control samples with the aim of identifying more candidate diagnostic biomarkers associated with PANoptosis in COPD. Five genes including *BOK, CD14, LY96, IL1B*, and *IRF2* were identified through the overlap of DEGs, WGCNA modules, and PANRGs.[43] Subsequent KEGG enrichment analysis found that these five genes were enriched to Pertussis, NF-kappa B signaling pathway, Tuberculosis and other KEGG pathways. It is worth noting that respiratory infections were more prevalent in COPD patients and Pertussis has been shown to exacerbate COPD progression.[44] The redox-sensitive transcription factor, nuclear factor kappa B played a crucial role in regulating cytokine activity within airway pathology and has been implicated in airway inflammation associated with asthma and COPD.[45] Yakar et al reported that Tuberculosis led to increased hospitalization rates and decreased respiratory function among COPD patients, COPD diagnosis and death occurred 5 years earlier in patients with Tuberculosis.[46] Therefore, we believe that the PANRGs were involved in the inflammatory responses of COPD. We further identified three candidate genes including *BOK, CD14*, and *IRF2* using LASSO regression and the SVM-RFE algorithm. Our stratified analysis by disease stage revealed that the positive correlations among *CD14, IRF2*, and *BOK* were specifically significant in late-stage COPD, whereas no such associations were observed in early-stage patients. This suggests that PANoptosis-related pathways may undergo potential dynamic recruitment during the late stages of COPD. Validation using three additional independent datasets consistently highlighted *CD14* as a key gene associated with COPD PANoptosis, showing significantly higher expression in COPD samples.

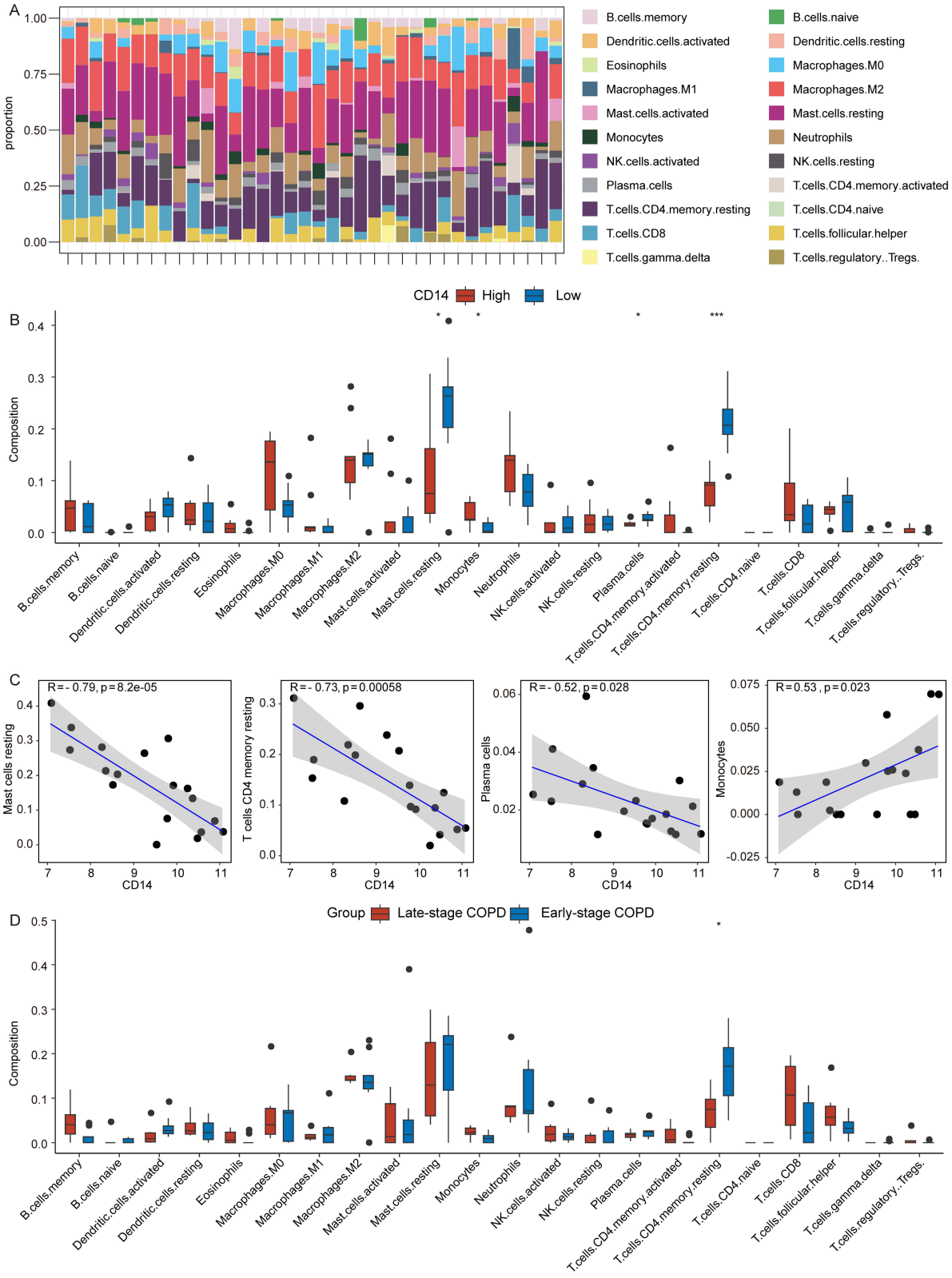

Figure 6 Evaluation of immune cell infiltration analysis in COPD. (**A**) Stacked plot of 22 immune infiltrating cells in each sample. (**B**) Box plot of 22 immune cell infiltration between high and low *CD14* expression groups. (**C**) Scatter plot of the correlation between *CD14* expression and significantly different immune cells. (**D**) Box plot of 22 immune cells infiltration between late-stage and early-stage COPD samples. Statistical significance: *P < 0.05, ***P < 0.001.

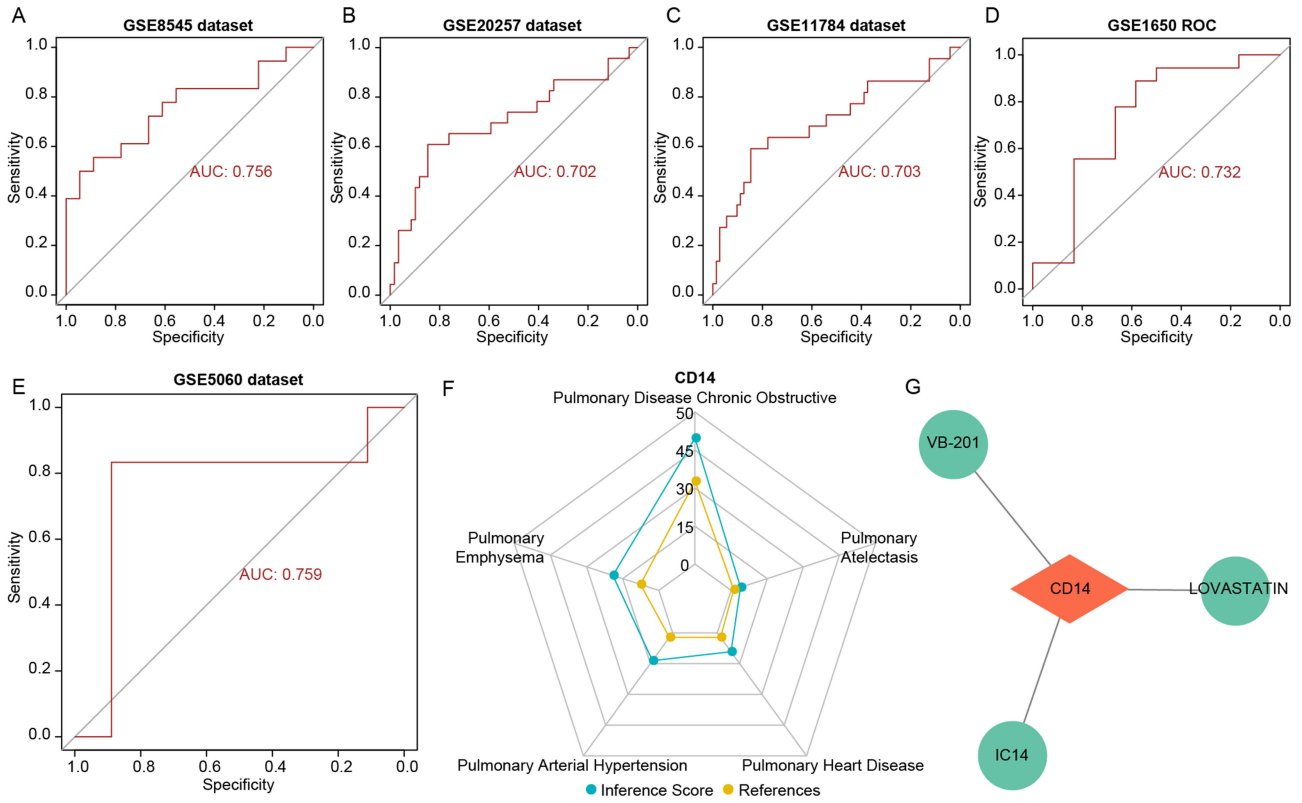

Figure 7 Clinical value mining and drug prediction of *CD14*. (**A–E**) The ROC curves of GSE8545, GSE20257, GSE11784, GSE1650 and GSE5060 cohorts. (**F**) Inference score radar map of *CD14* in COPD identified by CTD database. (**G**) *CD14* target drug network predicted by DGIdb database.

CD14 acts as a pivotal surface antigen mediating LPS-induced inflammation by orchestrating the activation of TLR4-dependent immune pathways.[47,48] As an early regulator of oxPAPC-induced hyperactivation, *CD14* predominantly mediates non-infectious inflammatory responses.[49] Multiple studies have reported elevated *CD14* expression in patients experiencing various acute infectious processes. For instance, CD14+ monocytes increased significantly in Controlling latent tuberculosis infection compared with healthy controls.[50] *CD14* was up-regulated in acute lung injury associated with sepsis, and inhibition of *CD14* expression could reduce the injury in patients.[51] In COVID-19, plasma concentrations of sCD14 increased significantly with the severity of the disease.[52] In addition, *CD14* had been reported to be involved in periodontitis[53] and influenza.[54] Nonetheless, recent studies have unveiled its more intricate regulatory roles in maintaining cellular and tissue immune homeostasis. Evidence suggests that membrane-bound *CD14* on macrophages plays a critical role in the clearance of apoptotic cells by recognizing outer membrane phospholipids.[55] Notably, recent proteomic evidence indicates that rather than functioning as a direct receptor for phosphatidylserine, the classical apoptotic signal, *CD14* recognizes externalized phosphoinositides (PIPs) as the authentic "eat-me" signals.[56] It is significant that PIPs are externalized and subsequently recognized by *CD14* regardless of whether the cell undergoes apoptosis, ferroptosis, or necroptosis.[57] Given that the crosstalk and coexistence of these diverse cell death modes constitute the foundation of PANoptosis, these findings may elucidate the potential reasons for the significant elevation of *CD14* within the PANoptosis-active pathological milieu of COPD. These findings suggest that *CD14* levels may, to some extent, serve as a potential indicator reflecting the scale of PANoptosis in the lung tissue of COPD patients. This could potentially assist clinicians in performing a preliminary assessment of parenchymal lung damage activity without necessarily resorting to invasive biopsy.

Next, we examined whether *CD14* has the potential to be a diagnostic biomarker for COPD. Our findings revealed that the proportion of immune cell infiltration, including T cells CD4 memory resting, plasma cells, and mast cells resting, were significantly lower in the *CD14* high expression group compared to the *CD14* low expression group. Among them, CD4 T cells play an important role in the immune system, protecting tissues from reinfection and cancer,

https://doi.org/10.2147/COPD.S577042

and are also involved in allergy, autoimmunity, graft rejection, and chronic inflammation.[58] Mast cells, as innate immune cells resident in tissues, play a key role in the inflammatory response and tissue homeostasis.[59] It is well known that inflammation occurs first in COPD. Based on these results, we hypothesized that *CD14* regulates the COPD process by participating in the inflammatory response. To make the results more convincing, we further succeeded in demonstrating that the proportion of immune infiltrates of T cells CD4 memory resting in the late COPD cohort was also significantly lower than that in the early COPD cohort. In addition, the diagnostic value of *CD14* was evaluated by ROC curve analysis, and the results showed that *CD14* had a good diagnostic effect on multiple data sets. This means that *CD14* may be used as a diagnostic marker for COPD in clinical practice. Compared with established COPD biomarkers such as SP-B reported by D'Ascanio et al, *CD14* demonstrates unique diagnostic potential.[60] SP-B is an organ-specific protein synthesized exclusively by alveolar type II cells, and its elevated plasma levels are primarily thought to indicate structural compromise of the alveolar-capillary barrier and direct parenchymal injury.[60] However, our findings suggest that *CD14* might be a more pivotal immunological driver in the progression of COPD. Unlike SP-B, which largely reflects anatomical damage and the resulting protein leakage, *CD14* was identified through high-resolution scRNA-seq and appears to function as a central hub orchestrating innate immune responses and chronic inflammation. Consequently, *CD14* may represent a promising biomarker that possesses deeper mechanistic support.

This study represents a translational research effort based on multi-omic integration and machine learning algorithms, aiming to systematically identify key regulatory factors associated with PANoptosis in COPD. Although we successfully identified and validated the potential of *CD14* as a critical diagnostic biomarker, several limitations remain to be addressed. The current research relies primarily on the retrospective analysis of public datasets and lacks validation from large-scale prospective clinical cohorts; furthermore, our findings highlight the potential of *CD14* as a diagnostic biomarker, the current study is descriptive and correlational in nature. We have not yet provided direct experimental evidence to demonstrate the precise clinical repercussions caused by *CD14* dysregulation. Whether the elevated expression of *CD14* is a driver of lung function decline or merely a molecular byproduct of the PANoptotic environment remains to be elucidated. Future mechanistic studies involving gene knockdown or overexpression in animal models are necessary to clarify the causal impact of *CD14* on COPD progression and its associated clinical outcomes.

Conclusions

In summary, this study systematically identified and validated the signature of PANoptosis-related hub genes, notably *CD14*, which exhibited significantly high expression in human COPD. By integrating multiple transcriptomic datasets and utilizing advanced machine learning algorithms, we demonstrated that these biomarkers possess high diagnostic accuracy, as further confirmed by ROC curve analysis. Furthermore, our PANoptosis-based model provides a more robust and comprehensive framework for understanding the dysregulation of the lung immune microenvironment. While these findings offer novel insights into the precision diagnosis of COPD, further large-scale prospective clinical trials and mechanistic experiments (both in vivo and in vitro) are warranted to validate their therapeutic potential and to elucidate the specific regulatory axes of these hub genes.

Data Sharing Statement

Data that support the findings of this study are openly available in Gene Expression Omnibus (GEO) at https://www.ncbi.nlm.nih.gov/geo, reference number GSE8545, GSE20257, GSE11784, and GSE173896.

Ethical Approval and Consent to Participate

In accordance with Article 32(1) of the Measures for Ethical Review of Life Science and Medical Research Involving Human Subjects, jointly issued by the National Health Commission, the Ministry of Education, the Ministry of Science and Technology, and the National Administration of Traditional Chinese Medicine on February 18, 2023, research conducted using "lawfully obtained publicly available data, or data generated through observation of public behavior without interfering with such behavior" may be exempt from ethical review. The dataset used in this study consists of lawfully obtained publicly available data. The research process does not cause harm to human subjects, does not involve

sensitive personal information, and does not involve commercial interests, thereby meeting the above criteria for exemption from ethical review.

Author Contributions

All authors made a significant contribution to the work reported, whether that is in the conception, study design, execution, acquisition of data, analysis and interpretation, or in all these areas; took part in drafting, revising or critically reviewing the article; gave final approval of the version to be published; have agreed on the journal to which the article has been submitted; and agree to be accountable for all aspects of the work.

Funding

The authors received no specific funding for this work.

Disclosure

The authors report no conflicts of interest in this work.

References

1. Sumbul H, Yuzer A. Design and implementation of a spirometric measurement system that can measure COPD parameters. *Pamukkale Univer J Engineer Sci*. 2022;28:661–667. doi:10.5505/pajes.2021.23835
2. Agusti A, Celli BR, Criner GJ, et al. Global initiative for chronic obstructive lung disease 2023 report: GOLD executive summary. *Am J Respir Crit Care Med*. 2023;207(7):819–837. doi:10.1164/rccm.202301-0106PP
3. Rabe KF, Watz H. Chronic obstructive pulmonary disease. *Lancet*. 2017;389(10082):1931–1940. doi:10.1016/S0140-6736(17)31222-9
4. Calverley PMA, Walker PP. Contemporary concise review 2022: chronic obstructive pulmonary disease. *Respirology*. 2023;28(5):428–436. doi:10.1111/resp.14489
5. Silvestri GA, Young RP. Strange bedfellows: the interaction between COPD and lung cancer in the context of lung cancer screening. *Ann Am Thorac Soc*. 2020;17(7):810–812. doi:10.1513/AnnalsATS.202005-433ED
6. Li X, Noell G, Tabib T, et al. Single cell RNA sequencing identifies IGFBP5 and QKI as ciliated epithelial cell genes associated with severe COPD. *Respir Res*. 2021;22(1):100. doi:10.1186/s12931-021-01675-2
7. Esther CR, O'Neal WK, Anderson WH, et al. Identification of sputum biomarkers predictive of pulmonary exacerbations in COPD. *Chest*. 2022;161(5):1239–1249. doi:10.1016/j.chest.2021.10.049
8. Zhong S, Yang L, Liu N, et al. Identification and validation of aging-related genes in COPD based on bioinformatics analysis. *Aging*. 2022;14(10):4336–4356. doi:10.18632/aging.204064
9. Chen H, Xia Z, Qing B, et al. Analysis of necroptosis-related prognostic genes and immune infiltration in idiopathic pulmonary fibrosis. *Front Immunol*. 2023;14:1119139. doi:10.3389/fimmu.2023.1119139
10. Ando F. Chemical preparation in endodontic therapy. 1. The effect of EDTA on powdered dentin and dentinal walls. *Aichi Gakuin Daigaku Shigakkai Shi*. 1985;23(2):448–454.
11. Song Q, Zhou A, Cheng W, et al. Bone marrow mesenchymal stem cells-derived exosomes inhibit apoptosis of pulmonary microvascular endothelial cells in COPD mice through miR-30b/Wnt5a pathway. *Int J Nanomed*. 2025;20:1191–1211. doi:10.2147/IJN.S487097
12. Wang R, Xu J, Wei S, Liu X. Increased Lipocalin 2 detected by RNA sequencing regulates apoptosis and ferroptosis in COPD. *BMC Pulm Med*. 2024;24(1):535. doi:10.1186/s12890-024-03357-3
13. Cao C, Zhong Z, Wu B, et al. Chronic exposure to cigarette smoke induces pyroptosis in pulmonary epithelial cells via EGR1/USP44/TRAF6 axis in COPD. *J Inflamm Res*. 2025;18:16619–16635. doi:10.2147/JIR.S546865
14. Xiao Y, Zhao C, Tai Y, et al. STING mediates hepatocyte pyroptosis in liver fibrosis by epigenetically activating the NLRP3 inflammasome. *Redox Biol*. 2023;62:102691. doi:10.1016/j.redox.2023.102691
15. Yu L, Guo Q, Li Y, et al. CHMP4C promotes pancreatic cancer progression by inhibiting necroptosis via the RIPK1/RIPK3/MLKL pathway. *J Adv Res*. 2025;77:653–668. doi:10.1016/j.jare.2025.01.040
16. Mizumura K, Ozoe R, Nemoto Y, et al. Cigarette smoke extract-induced necroptosis causes mitochondrial DNA release and inflammation of bronchial epithelial cells. *Int J Chron Obstruct Pulmon Dis*. 2025;20:2685–2695. doi:10.2147/COPD.S523610
17. Dejas L, Santoni K, Meunier E, Lamkanfi M. Regulated cell death in neutrophils: from apoptosis to NETosis and pyroptosis. *Semin Immunopathol*. 2023;70:101849. doi:10.1016/j.smim.2023.101849
18. Chen S, Jiang J, Li T, Huang L. PANoptosis: mechanism and role in pulmonary diseases. *Int J Mol Sci*. 2023;24(20).
19. Samir P, Malireddi RKS, Kanneganti TD. The PANoptosome: a deadly protein complex driving pyroptosis, apoptosis, and necroptosis (PANoptosis). *Front Cell Infect Microbiol*. 2020;10:238. doi:10.3389/fcimb.2020.00238
20. Malireddi RKS, Kesavardhana S, Kanneganti TD. ZBP1 and TAK1: master regulators of NLRP3 inflammasome/pyroptosis, apoptosis, and necroptosis (PAN-optosis). *Front Cell Infect Microbiol*. 2019;9:406. doi:10.3389/fcimb.2019.00406
21. Christgen S, Zheng M, Kesavardhana S, et al. Identification of the PANoptosome: a molecular platform triggering pyroptosis, apoptosis, and necroptosis (PANoptosis). *Front Cell Infect Microbiol*. 2020;10:237. doi:10.3389/fcimb.2020.00237
22. Malireddi RKS, Kesavardhana S, Karki R, Kancharana B, Burton AR, Kanneganti TD. RIPK1 distinctly regulates yersinia-induced inflammatory cell death, PANoptosis. *Immunohorizons*. 2020;4(12):789–796. doi:10.4049/immunohorizons.2000097

23. Zheng M, Karki R, Vogel P, Kanneganti TD. Caspase-6 is a key regulator of innate immunity, inflammasome activation, and host defense. *Cell*. 2020;181(3):674–687e613. doi:10.1016/j.cell.2020.03.040
24. Malireddi RKS, Gurung P, Kesavardhana S, et al. Innate immune priming in the absence of TAK1 drives RIPK1 kinase activity-independent pyroptosis, apoptosis, necroptosis, and inflammatory disease. *J Exp Med*. 2020;217(3). doi:10.1084/jem.20191644
25. Zhou R, Ying J, Qiu X, et al. A new cell death program regulated by toll-like receptor 9 through p38 mitogen-activated protein kinase signaling pathway in a neonatal rat model with sepsis associated encephalopathy. *Chinese Med J*. 2022;135(12):1474–1485. doi:10.1097/CM9.0000000000002010
26. Karki R, Lee S, Mall R, et al. ZBP1-dependent inflammatory cell death, PANoptosis, and cytokine storm disrupt IFN therapeutic efficacy during coronavirus infection. *Sci Immunol*. 2022;7(74):eabo6294. doi:10.1126/sciimmunol.abo6294
27. Lee S, Karki R, Wang Y, Nguyen LN, Kalathur RC, Kanneganti TD. AIM2 forms a complex with pyrin and ZBP1 to drive PANoptosis and host defence. *Nature*. 2021;597(7876):415–419. doi:10.1038/s41586-021-03875-8
28. Karki R, Sharma BR, Tuladhar S, et al. Synergism of TNF-alpha and IFN-gamma triggers inflammatory cell death, tissue damage, and mortality in SARS-CoV-2 infection and cytokine shock syndromes. *Cell*. 2021;184(1):149–168e117. doi:10.1016/j.cell.2020.11.025
29. Messaoud-Nacer Y, Culerier E, Rose S, et al. STING agonist diABZI induces PANoptosis and DNA mediated acute respiratory distress syndrome (ARDS). *Cell Death Dis*. 2022;13(3):269. doi:10.1038/s41419-022-04664-5
30. Nisa A, Kipper FC, Panigrahy D, Tiwari S, Kupz A, Subbian S. Different modalities of host cell death and their impact on Mycobacterium tuberculosis infection. *Am J Physiol Cell Physiol*. 2022;323(5):C1444–C1474. doi:10.1152/ajpcell.00246.2022
31. Tilley AE, O'Connor TP, Hackett NR, et al. Biologic phenotyping of the human small airway epithelial response to cigarette smoking. *PLoS One*. 2011;6(7):e22798. doi:10.1371/journal.pone.0022798
32. Shaykhiev R, Otaki F, Bonsu P, et al. Cigarette smoking reprograms apical junctional complex molecular architecture in the human airway epithelium in vivo. *Cell Mol Life Sci*. 2011;68(5):877–892. doi:10.1007/s00018-010-0500-x
33. Ammous Z, Hackett NR, Butler MW, et al. Variability in small airway epithelial gene expression among normal smokers. *Chest*. 2008;133(6):1344–1353. doi:10.1378/chest.07-2245
34. Langfelder P, Horvath S. WGCNA: an R package for weighted correlation network analysis. *BMC Bioinf*. 2008;9:559. doi:10.1186/1471-2105-9-559
35. Ritchie ME, Phipson B, Wu D, et al. limma powers differential expression analyses for RNA-sequencing and microarray studies. *Nucleic Acids Res*. 2015;43(7):e47. doi:10.1093/nar/gkv007
36. Yu G, Wang LG, Han Y, He QY. clusterProfiler: an R package for comparing biological themes among gene clusters. *Omics*. 2012;16(5):284–287. doi:10.1089/omi.2011.0118
37. Friedman J, Hastie T, Tibshirani R. Regularization paths for generalized linear models via coordinate descent. *J Stat Softw*. 2010;33(1):1–22. doi:10.18637/jss.v033.i01
38. Szklarczyk D, Gable AL, Lyon D, et al. STRING v11: protein-protein association networks with increased coverage, supporting functional discovery in genome-wide experimental datasets. *Nucleic Acids Res*. 2019;47(D1):D607–D613. doi:10.1093/nar/gky1131
39. Shannon P, Markiel A, Ozier O, et al. Cytoscape: a software environment for integrated models of biomolecular interaction networks. *Genome Res*. 2003;13(11):2498–2504. doi:10.1101/gr.1239303
40. Hao Y, Hao S, Andersen-Nissen E, et al. Integrated analysis of multimodal single-cell data. *Cell*. 2021;184(13):3573–3587e3529. doi:10.1016/j.cell.2021.04.048
41. Newman AM, Liu CL, Green MR, et al. Robust enumeration of cell subsets from tissue expression profiles. *Nat Methods*. 2015;12(5):453–457. doi:10.1038/nmeth.3337
42. Obuchowski NA, Bullen JA. Receiver operating characteristic (ROC) curves: review of methods with applications in diagnostic medicine. *Phys Med Biol*. 2018;63(7):07TR01. doi:10.1088/1361-6560/aab4b1
43. Zhang B, Huang B, Zhang X, et al. PANoptosis-related molecular subtype and prognostic model associated with the immune microenvironment and individualized therapy in pancreatic cancer. *Front Oncol*. 2023;13:1217654. doi:10.3389/fonc.2023.1217654
44. Aris E, Harrington L, Bhavsar A, et al. Burden of pertussis in COPD: a retrospective database study in England. *COPD*. 2021;18(2):157–169. doi:10.1080/15412555.2021.1899155
45. Schuliga M. NF-kappaB signaling in chronic inflammatory airway disease. *Biomolecules*. 2015;5(3):1266–1283. doi:10.3390/biom5031266
46. Yakar HI, Gunen H, Pehlivan E, Aydogan S. The role of tuberculosis in COPD. *Int J Chron Obstruct Pulmon Dis*. 2017;12:323–329. doi:10.2147/COPD.S116086
47. Wu Z, Zhang Z, Lei Z, Lei P. CD14: biology and role in the pathogenesis of disease. *Cytokine Growth Factor Rev*. 2019;48:24–31. doi:10.1016/j.cytogfr.2019.06.003
48. Ciesielska A, Matyjek M, Kwiatkowska K. TLR4 and CD14 trafficking and its influence on LPS-induced pro-inflammatory signaling. *Cell Mol Life Sci*. 2021;78(4):1233–1261.
49. Zanoni I, Tan Y, Di Gioia M, Springstead JR, Kagan JC. By capturing inflammatory lipids released from dying cells, the receptor CD14 induces inflammasome-dependent phagocyte hyperactivation. *Immunity*. 2017;47(4):697–709e693. doi:10.1016/j.immuni.2017.09.010
50. Wang PH, Wu MF, Hsu CY, et al. The dynamic change of immune checkpoints and CD14+ monocytes in latent tuberculosis infection. *Biomedicines*. 2021;9(10). doi:10.3390/biomedicines9101479
51. Ju N, Hayashi H, Shimamura M, et al. Prevention of acute lung injury by a novel CD14-inhibitory receptor activator of the NF-kappaB ligand peptide in mice. *Immunohorizons*. 2021;5(6):438–447. doi:10.4049/immunohorizons.2000112
52. Messner CB, Demichev V, Wendisch D, et al. Ultra-High-Throughput clinical proteomics reveals classifiers of COVID-19 infection. *Cell Syst*. 2020;11(1):11–24e14. doi:10.1016/j.cels.2020.05.012
53. Fageeh HN, Fageeh HI, Khan SS, et al. Gingival crevicular fluid infiltrating CD14+ monocytes promote inflammation in periodontitis. *Saudi J Biol Sci*. 2021;28(5):3069–3075. doi:10.1016/j.sjbs.2021.02.049
54. Wong SS, Oshansky CM, Guo XJ, et al. Activated CD4(+) T cells and CD14(hi)CD16(+) monocytes correlate with antibody response following influenza virus infection in humans. *Cell Rep Med*. 2021;2(4):100237. doi:10.1016/j.xcrm.2021.100237
55. Devitt A, Pierce S, Oldreive C, Shingler WH, Gregory CD. CD14-dependent clearance of apoptotic cells by human macrophages: the role of phosphatidylserine. *Cell Death Differ*. 2003;10(3):371–382. doi:10.1038/sj.cdd.4401168

56. Kim OH, Kang GH, Hur J, et al. Externalized phosphatidylinositides on apoptotic cells are eat-me signals recognized by CD14. *Cell Death Differ*. 2022;29(7):1423–1432. doi:10.1038/s41418-022-00931-2
57. Na K, Oh BC, Jung Y. Multifaceted role of CD14 in innate immunity and tissue homeostasis. *Cytokine Growth Factor Rev*. 2023;74:100–107. doi:10.1016/j.cytogfr.2023.08.008
58. Kunzli M, Masopust D. CD4(+) T cell memory. *Nat Immunol*. 2023;24(6):903–914. doi:10.1038/s41590-023-01510-4
59. Aponte-Lopez A, Munoz-Cruz S. Mast cells in the tumor microenvironment. *Adv Exp Med Biol*. 2020;1273:159–173.
60. D'Ascanio M, Viccaro F, Pizzirusso D, et al. Surfactant protein B plasma levels: reliability as a biomarker in COPD patients. *Biomedicines*. 2023;11(1):124. doi:10.3390/biomedicines11010124